JOURNAL OF MATERIALS SCIENCE 16 (1981) 3093–3098

Kinetics of densification during hot-pressing of aluminium nitride

J-P. LECOMPTE, J. JARRIGE, J. MEXMAIN
Centre de Recherches et d'Études Céramiques, Equipe de recherche associée au CNRS, University of Limoges, Limoges 87060, France

R. J. BROOK, F. L. RILEY
Department of Ceramics, University of Leeds, Leeds, UK

Aluminium nitride powder has been hot-pressed at 1700° C under pressures in the range 5 to 30 MPa, and with additions of small weight percentages of alumina. Analysis of the densification kinetics shows two regimes. For pressures below 24 MPa the stress exponent of the densification rate is approximately 1.0 and the grain-size exponent is approximately 3, suggesting that grain-boundary diffusion is rate controlling. For pressures above 24 MPa the stress exponent is approximately 10, indicative of dislocation creep. At low pressures the existence of a threshold stress is apparent, values of which vary with the second-phase volume.

1. Introduction

Fully-dense aluminium nitride ceramics have excellent thermal and mechanical properties [1] and also perform well under high applied pressures [2]. These features make them good candidates for high-temperature and high-stress engineering applications [3–5]. In addition, aluminium nitride has excellent high-temperature dielectric properties and good high-temperature chemical stability in contact with metals [6, 7] and carbon.

It is difficult to make high-purity aluminium nitride free from oxygen contamination, and it is now recognized that an oxygen content of about 2 weight per cent is necessary for sintering to full density [8, 9]. The oxide film on the surface of the aluminium nitride powder particles reacts with the aluminium nitride to form aluminium oxynitride during hot-pressing under pressure of 30 to 40 MPa in carbon dies at temperatures of 1900° C and above [10]. The rôle of oxygen in the densification process has, however, not yet been clarified. The object of this study has therefore been to investigate, in detail, the kinetics of the densification of aluminium nitride during pressure sintering, with particular regard to the determination of the densification mechanism, and the possible involvement of liquid phase.

2. Experimental procedure

2.1. Materials

Commercial aluminium nitride* and alumina† powders were used. Neutron activation analysis of the aluminium nitride revealed the presence of 2.7 wt% oxygen. Particle-size analysis (conducted using a sedigraph manufactured by Micromeritics) showed that the apparent mean grain size was 16 μm. For this study, a powder fraction obtained by sieving the aluminium nitride in petroleum ether was used, with an apparent mean grain size of 9 μm. The specific surface area of this powder measured by BET (using a Perkin–Elmer shell-model 212 D Sorptometer) was, however, 2.7 $m^2 g^{-1}$, the individual mean spherical grain size calculated on the basis of this value being 0.7 μm. Scanning electron microscopy showed that the grains were in fact non-spherical agglomerates.

In order to obtain a powder of different grain size, batches of aluminium nitride powder (10 g)

*AlN: 99% pure, 50 μm nominal mean particle size; obtained from Koch–Light Laboratories, Colnbrook, Bucks., UK.
†$Al_2O_3\alpha$: 99.99% pure, 0.3 μm nominal mean particle size; obtained from Linde Aktien Ges., Wiesbaden, Germany.

0022–2461/81/113093–6$02.60/0

and propan-2-ol (25 cm^3) were milled using a vibromill for 90 min in a polyethylene container with alumina grinding pellets. Contamination of the nitride occurred, the extent of which was determined from measurements of weight-loss of the pellets (approximately 3 wt% Al_2O_3). The specific surface area was now 3.3 $m^2\ g^{-1}$, equivalent to an average grain size 0.5 μm. The true grain-size ratio between the two powders was therefore 1.4.

2.2. Procedure

The hot-pressing apparatus, its associated control and monitoring equipment, and general procedure has been described in detail elsewhere [11]. In order to avoid reaction between the aluminium nitride and the graphite die (of 12.7 mm internal diameter) at high temperature, the die interior and the graphite spacer dies were coated with a thin wash of high-purity boron nitride suspended in an aqueous solution of methyl cellulose. 3 g of the aluminium nitride powder were used for each pressing. Pressures of 5 to 30 MPa were used. The density of each pressed pellet was measured with a Doulton mercury densitometer.

3. Results

Hot-pressings were carried out at 1700° C. The applied pressure was varied over the range 5 to 30 MPa. Rates of densification were calculated for various densities by taking the gradient of the density–time plots for each pressing.

3.1. Dependence of the densification rate on the applied pressure

Instantaneous densification rates ($d\rho/dt$) for the 0.5 and 0.7 μm powders at $\rho/\rho_\infty = 0.8$, calculated from the density (ρ)–time (t) curves, are plotted in Fig. 1 as a function of pressure (MPa). It can be seen that there are two regimes covering the applied stress ranging from 5 to 25 MPa, and from 24 to 30 MPa; in the latter range the densification rate is very fast. The densification behaviour can be described in terms of the relationship

$$d\rho/dt = K(\sigma - \sigma_0)^n, \qquad (1)$$

where n is the stress exponent, K is a constant and σ_0 is the threshold stress, i.e., the value for which $d\rho/dt = 0$ at $\rho/\rho_\infty = 0.80$.

In Fig. 2 $\log d\rho/dt$ is plotted as a function of $\log_{10}(\sigma - \sigma_0)$. In the range of 5 to 24 MPa the stress exponent, n, is approximately 1.0 and in

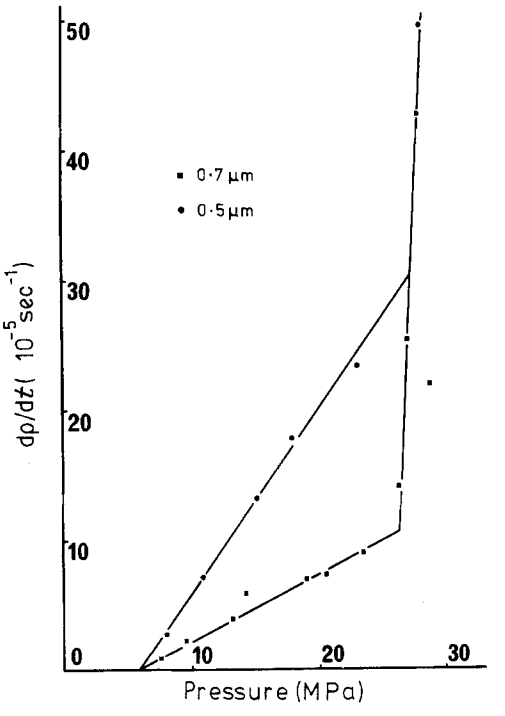

Figure 1 Instantaneous (relative) densification rates at a relative density of 0.80 for two aluminium nitride powders, plotted as a function of applied pressure. Hot-pressing temperature 1700° C.

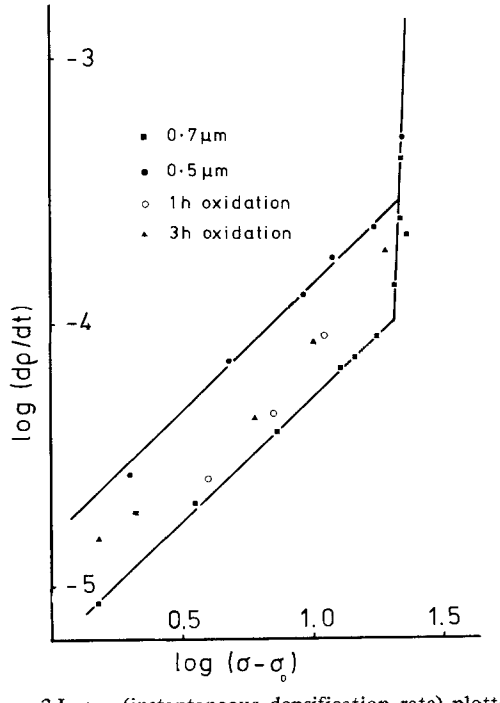

Figure 2 Log_{10} (instantaneous densification rate) plotted as a function of $\log_{10}$ (applied pressure) with compensation for apparent threshold stress. Data taken from Figs 1 and 4.

the range from 24 to 30 MPa n is of the order of 10.

3.2. Dependence of the rate of densification on the grain size

Also shown in Fig. 1 is the densification behaviour of the 0.5 μm powder. It can be seen that in the pressure range 5 to 24 MPa the instantaneous densification rate also depends linearly on applied stress. The actual rates of densification are however higher. Fig. 2 shows, in the range 5 to 24 MPa, a stress exponent, n, of 1.0, and, in the range 24 to 30 MPa, a stress exponent of 10. The densification-rate ratio between the two powders in the lower stress region is 2.7.

3.3. Dependence of the rate of densification on the second-phase content

3.3.1. 5 wt % addition of alumina powder

5 wt % of alumina was mixed with the aluminium nitride using an agate mortar and pestle. It is seen in Fig. 3 that these additions of alumina did not change significantly the rate of densification. Essentially the same stress dependence for densification was also obtained.

3.3.2. Oxidation of the aluminium nitride powder

The work of Tetard and Billy [12] shows that, for an aluminium nitride powder identical to that used in this study, oxidation of 25% takes place after heating at 900° C for 10 h. The aluminium nitride powder was accordingly oxidized in a muffle furnace for different lengths of time (1 h and 3 h) at 800° C and neutron activation analysis was conducted on the powders for 1 h and 3 h which indicated that they contained 6.45 and 14.2 wt % of oxygen, respectively. The hot-pressing densification behaviour of these powders, shown in Fig. 4, is significantly different in that σ_0, the threshold stress, is now increased to 8 and 10 MPa for the 6.45 and 14.2 wt % O_2 powders, respectively. Fig. 2 shows that the densification rate in the low-stress regime is also increased. The stress exponent, however, remains unchanged at 1.0.

3.4. Discussion

Analysis of the densification kinetics in terms of the hot-pressing equation presented by Sakai and Iwata [13]

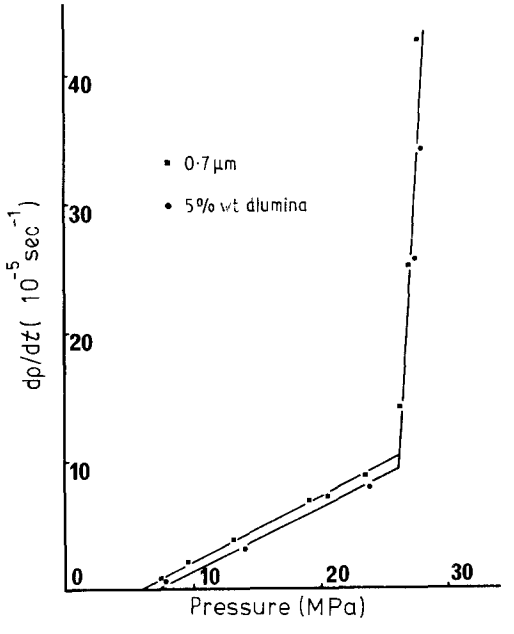

Figure 3 Instantaneous (relative) densification rates at a relative density of 0.80 for 0.7 μm grain size aluminium nitride powder and for powder containing 5 wt % alumina powder, plotted as a function of applied pressure. Hot-pressing temperature 1700° C.

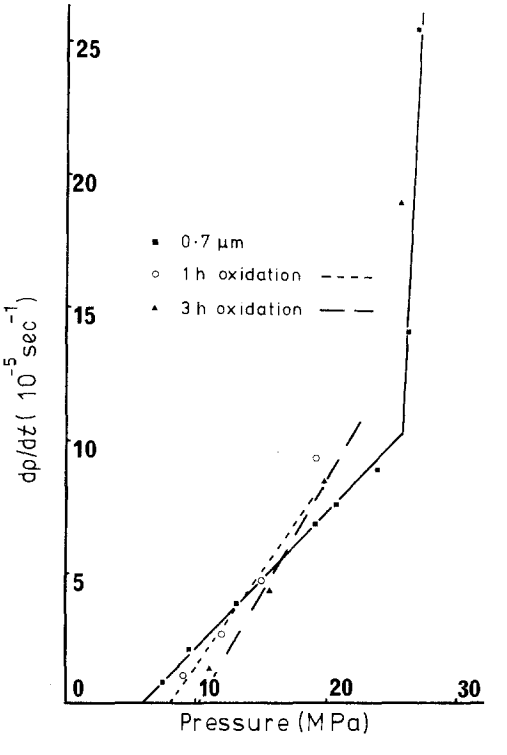

Figure 4 Instantaneous (relative) densification rates at a relative density of 0.80 for 0.7 μm grain size aluminium nitride powder, and for powders oxidized for 1 and 3 h, plotted as a function of applied pressure. Hot-pressing temperature 1700° C.

$$-\ln(1-p) = \frac{9}{2}\frac{40D\Omega}{kTd^2}(\sigma_2-\sigma_1)t - \ln(1-p_0), \quad (2)$$

(where ρ is the relative porosity at time t, p_0 is the initial relative porosity, D is the self-diffusion coefficient, T is the absolute temperature, k is Boltzmann's constant, Ω is the atomic volume of the rate-controlling species, d is the mean grain size and $\sigma_2 - \sigma_1$ is the difference between the applied pressure and the gas pressure in the pores) has not proved helpful because the relation between $\ln(p/p_0)$ and t is not linear. It has been decided, therefore, to use the well-established procedure of comparing the experimental stress exponent of the densification rate with the values predicted by theoretical models. Examples of n-values for different creep and sintering densification mechanisms are listed in [17].

In the present case the stress exponent for the low-pressure regime is $n \sim 1.0$; above 24 MPa the exponent increases to $n \approx 10$. These certain exponent variations have been observed in the creep of certain ceramics by Burton [14] and Coath and Wilshire [15]. For the high-pressure regime they have established, from a comparison with theoretical stress exponents, that creep is a result of the generation and movement of dislocations. In the low-stress range, the stress dependence has generally been considered in terms of stress-directed vacancy diffusion either through the lattice (Nabarro–Herring creep) or along the grain boundaries (Coble creep). If diffusion is of the lattice type the rate of densification, $\dot{\epsilon}$, follows a law

$$\dot{\epsilon} = \frac{k_1 D_L \Omega \sigma}{kTd^2}, \quad (3)$$

where d is the grain size, D_L is the lattice diffusion coefficient and Ω is the atomic volume of the diffusing species. If grain-boundary diffusion (Coble creep) is rate controlling, the rate of densification, $\dot{\epsilon}$, follows a law

$$\dot{\epsilon} = \frac{k_2 D_b w \Omega \sigma}{kTd^3}, \quad (4)$$

where D_b is the grain-boundary diffusion coefficient, w is the grain-boundary width, k_1 and k_2 are numerical constants and k is Boltzmann's constant.

For both processes the relation between $\dot{\epsilon}$ and σ is linear. Thus, for a grain-size exponent of 2 in the low-pressure region the indicated process is that of lattice diffusion; a grain-size exponent of 3 would suggest Coble creep with grain-boundary transport of material. Fig. 2 shows that the instantaneous rate of densification increases by a factor about 2.7 when the grain size is increased by a factor of 1.4. Thus,

$$\frac{\dot{\epsilon}_2}{\dot{\epsilon}_1} = 2.7 = \left(\frac{d_1}{d_2}\right)^{n'} = (1.4)^{n'} \quad (5)$$

and, hence,

$$n' \approx 3$$

where the subscripts 1 and 2 refer to the powders with mean grain sizes of 0.7 and 0.5 μm, respectively.

If, in the low-stress range, densification is controlled by grain-boundary diffusion, the rate of densification will be increased by increasing the thickness of the oxide film around the grains; the addition of alumina powder (Fig. 2) shows no such effect. The alternative approach of introducing oxide by oxidation of the powder is, however, a better test since it has been shown [12] that oxidation, beginning with a preferential attack of the asperities of the nitride particles and with the formation of many superficial dendrites, eventually leads to the blocking of pores and the formation of a protective oxide film. From Fig. 2, it is seen that the densification rates after such oxidiation increase in the low-pressure range. It therefore seems probable that the controlling mechanism for the densification is diffusion in these alumina films around the grains. In the pseudo-binary Al_2O_3–AlN, McCauley [16] finds a liquid phase; in this system there seems, however, to be an intimate relation between liquid formation and the appearance of the various poly-types. Some of these are metastable and it can be difficult to differentiate between the presence of a liquid and that of the poly-types. Consequently, it is not possible to confirm that the grain-boundary phase of high diffusivity, believed to be responsible for the hot-pressing densification behaviour of aluminium nitride, is in fact a liquid.

In Fig. 3 the variation of the threshold stress with the different volume fractions of alumina can be seen. Other materials also exhibit variation of the σ_0 value with variation of a second-phase volume fraction. For the explanation of this threshold stress, Ashby [18] uses the interaction that will exist between boundary dislocations and second-phase particles lying in the boundary. In this case creep is possible if

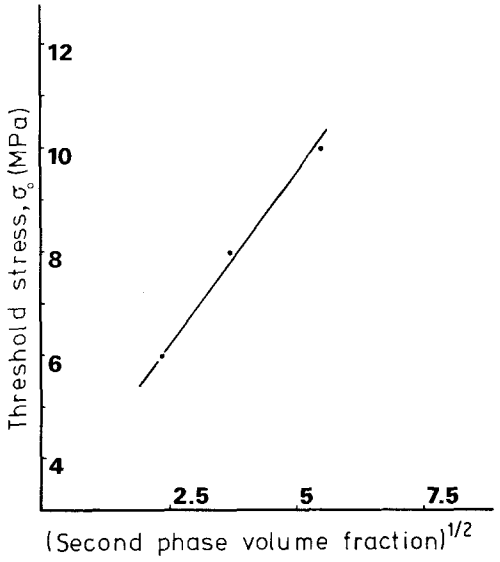

Figure 5 Threshold stress for a relative density of 0.80 plotted as a function of (volume-fraction alumina)$^{1/2}$, for 0.7 μm grain size aluminium nitride powder hot-pressed at 1700° C.

$$\sigma > \frac{2E}{\mathbf{b}\lambda}, \qquad (6)$$

where E is the line defect energy, **b** is the Burger's vector and λ is the second-phase spacing.

Burton [14] has discussed the different explanations for the threshold stress. A number of theories predict a linear variation of the threshold stress with the volume-fraction of the second-phase. Data for Au–Al_2O_3 and Cu–Al_2O_3 have given support to this theory of behaviour. Experimental results also give support to the theories which emphasise the particular importance of the presence of second-phase in the grain-boundary. In the present results (see Fig. 5), the threshold stress observed is, if anything, proportional to $V^{1/2}$ where V is the volume-fraction of particles in the second phase; this is the dependence proposed by the Ashby model. While this theory, which considers the interaction of grain-boundary line defects and second-phase particles, requires a threshold stress proportional to $V^{1/2}$, it is difficult to be persuaded that the complex phase relationships suggested for the alumina-rich materials in the Al–N–O system [16] are likely to yield readily the isolated second-phase particles conceived by the Ashby model. A high-resolution microstructural study of the grain boundaries in aluminium nitride would be helpful in resolving this question of the basis for the threshold stress.

4. Conclusions

The densification behaviour of aluminium nitride powders during hot-pressing at 1700° C is consistent with diffusion through a grain-boundary phase being rate-controlling for applied pressures of less than 24 MPa, and with dislocation creep being dominant for higher pressures. The grain-boundary oxide phase appears to be more effectively distributed throughout the system by means of a preliminary oxidation treatment, than by the additions of oxide powder.

Acknowledgements

Financial support provided by the British Council to J-PL is gratefully acknowledged, as is the interest and encouragement of Professor M. Billy. The authors are also indebted to Dr E. Gilbart for providing invaluable advice and experimental assistance with the hot-press facility.

References

1. P. BOCH, J. C. GLANDUS, J. JARRIGE, J. P. LECOMPTE and J. MEXMAIM, *Ceramurgia Int.*, to be published.
2. H. C. HEARD and C. F. CLINE, *J. Mater. Sci.* **15** (1980) 1889.
3. K. KOMEYA and F. NODA, Society of Automotive Engineers Paper Number 740239, 1974.
4. T. SAKAI, M. KURIYAMA, F. INUKAI and T. KIZIMA, *Nat. Inst. Res. Inorg. Mater.* **4** (1978) 174.
5. K. KOMEYA and F. NODA, *Toshiba Rev.* **92** (1974) 13.
6. H. KOTSCH and G. PUTZKY, *Abh. Deut. Akad. Wiss. Berlin, kl. Math. Phys. Tech.* 1 (1966) 249.
7. M. TRONTELJ and D. KOLAR, *J. Amer. Ceram. Soc.* **61** (1978) 204.
8. G. A. SLACK, GEC, Schenectady, New York, private communication.
9. T. SAKAI and I. M. IWATA, *J. Mater. Sci.* **12** (1977) 1659.
10. S. PROCHAZKA and C. F. BOBIK, *Sintering Prog.* **13** (1979) 321.
11. R. J. WESTON and T. G. CARRUTHERS, *Proc. Brit. Ceram. Soc.* **22** (1973) 197.
12. D. TETARD and M. BILLY, Proceedings of the 25th International Meeting of the Physical Chemistry Society, Dijon, France, July 1974, edited by P. Barret (Elsevier, Amsterdam, New York and Oxford, 1975) p. 512.
13. T. SAKAI and M. IWATA, *Jap. J. Appl. Phys.* **15** (1976) 537.
14. B. BURTON, "Diffusion and Defect Monograph Series: Diffusional Creep of Polycrystalline Materials" (Trans. Technical Publications, Aedermannsdorf, Switzerland, 1977) pp. 18–21, 68–78.
15. J. A. COATH and B. WILSHIRE, *Ceramurgia Int.* **3** (1977) 103.

16. J. W. McCAULEY and N. D. CORBIN, *J. Amer. Ceram. Soc.* **62** (1979) 476.
17. M. N. A. RAHAMAN, F. L. RILEY and R. J. BROOK, *J. Amer. Ceram. Soc.* **65** (1980) 648.
18. M. F. ASHBY, *Surface Sci.* **1** (1972) 526.

Received 23 March and accepted 13 April 1981.